

Linking Spontaneous Activity of Single Cortical Neurons and the Underlying Functional Architecture

M. Tsodyks, T. Kenet, A. Grinvald,* A. Arieli

The relation between the activity of a single neocortical neuron and the dynamics of the network in which it is embedded was explored by single-unit recordings and real-time optical imaging. The firing rate of a spontaneously active single neuron strongly depends on the instantaneous spatial pattern of ongoing population activity in a large cortical area. Very similar spatial patterns of population activity were observed both when the neuron fired spontaneously and when it was driven by its optimal stimulus. The evoked patterns could be used to reconstruct the spontaneous activity of single neurons.

Cortical neurons are spontaneously active in the absence of external input even in primary sensory areas (1). Analogously, dynamic patterns of ongoing population activity sweep across the cortex, as recently demonstrated by high-resolution optical imaging (2). The spontaneous firing of neocortical neurons is often considered to be a noisy, stochastic process (3). A common assumption is that the stochastic activity of neighboring neurons is uncorrelated, which permits the averaging out of this noise. However, local field potentials and recordings from single neurons indicate the presence of highly synchronous ongoing activity patterns (4). Furthermore, we have shown in anesthetized cats (5) that the spontaneous activity of a single cortical neuron is highly correlated with the population activity in a large cortical area containing millions of neurons. We inquired if there is a relation between the ongoing patterns of cortical population activity that occur simultaneously with the action potentials of a single neuron, and the reproducible pattern of evoked activity shaped by the presentation of a well-defined optimal stimulus. We refer to these patterns as the spontaneous and evoked cortical states, respectively. A given evoked cortical state can be experimentally determined if signal averaging is used to remove the ever-changing ongoing activity from the individual responses to repeated presentation of that same stimulus. The pattern of evoked cortical activity for a particular stimulus attribute, such as a given orientation, and the functional map (that is, functional architec-

ture) related to this stimulus attribute are identical. Real-time optical imaging based on voltage-sensitive dyes is a useful tool for imaging the membrane potential changes of neuronal populations (6, 7). This technique (Fig. 1A) provides an accurate real-time view of neuronal activity spread across several neocortical hypercolumns, whose task is to process the visual input. Simultaneous recordings of single-unit activity and real-time optical imaging from a surrounding region were performed in areas 17 and 18 of the visual cortex of anesthetized cats (8). These allowed us to study the relation between the probability that a neuron will fire an action potential, and the pattern of the population activity in that region of the cortex, both in the presence and in the absence of visual input.

We first searched for neurons exhibiting a relatively high rate of spontaneous activity when the animal's eyes were closed (9). Next, we characterized the orientation tuning properties of these neurons and selected the neurons with sharp tuning preference and robust response. We chose orientation tuning as the specific functional property because the majority of neurons in cat striate cortex are tuned for the orientation of bars or gratings (10). Furthermore, the functional architecture and intracortical circuitry underlying orientation tuning are well known (11). We then performed simultaneous optical imaging and single-unit recordings for a period of 30 to 70 s during which a drifting grating of optimal orientation was presented (12). To determine the pattern of the evoked cortical state for which the neuron has a maximal firing rate, we averaged over all patterns observed at the times corresponding to action potentials that were evoked by the optimal stimulus (5). The spatial pattern thus observed is illustrated in Fig. 1C. We refer to such a spatial pattern as the neuron's pre-

ferred cortical state (PCS) (13). We then calculated the single condition orientation map from the same data by triggering the spatial patterns of activity on the time of stimulus onset. Not surprisingly, we found that the neuron's PCS pattern was very similar to the functional architecture map of the orientation columns illustrated in Fig. 1D (14).

We evaluated the similarity between every spatial pattern of population activity and the neuron's PCS. As a measure of the similarity between the two patterns, we used their correlation coefficient. We then compared the observed spike train (green bars) and the time course of the similarity (red trace, Fig. 2A). Each presentation of the optimal stimulus evoked increased spiking activity (bursts) and, as expected, the pattern of population activity became more similar to the neuron's PCS, as reflected by higher values of correlation coefficients (15). Another way of assessing the resemblance between the discrete spike train (green) and the continuous correlation trace (red) is to reconstruct a spike train (blue) from the correlation trace (16). Evidently, the two spike trains are similar. This procedure predicted well the occurrence of bursts in the observed spike train rather than the exact timing of single action potentials. Even in the absence of a stimulus, the neuron still tended to fire when the instantaneous cortical state was most similar to the neuron's PCS (Fig. 2B). The observed and reconstructed spike trains were similar; the bursts and sometimes even single action potentials concurred with the upswings in the value of the correlation between these two patterns. Thus, the spontaneous activity of the neuron could to a large extent be reconstructed from the time course of the similarity between the population activity and the neuron's PCS. It is important to emphasize that the PCS of the neuron was computed from an evoked recording session. These results imply that the spatial pattern revealed by computing the PCS of a neuron, and the spontaneous cortical state obtained by averaging over times corresponding to spontaneous action potentials, should be similar. Figure 2, C and D, illustrate that these two spatial patterns are indeed very similar (17). An example from a different animal is presented in Fig. 2, E and F. Because the PCS obtained during activation is similar to the functional architecture (Fig. 1, C and D), these results indicate that the spontaneous activity of cortical neurons depends on the underlying functional architecture associated with their tuning properties (18). The fact that the same states appeared during both spontaneous and evoked activity of the neurons also suggests that even in the presence of sensory inputs, the response of cortical neurons is affected by dynamically switching cortical states and is not only a direct reflection of the input.

Department of Neurobiology and the Center for Studies of Higher Brain Functions, Weizmann Institute of Science, Rehovot 76100, Israel.

*To whom correspondence should be addressed at the Weizmann Institute of Science, Department of Neurobiology, Post Office Box 26, Rehovot 76100, Israel. E-mail: bngrinva@weizmann.weizmann.ac.il

REPORTS

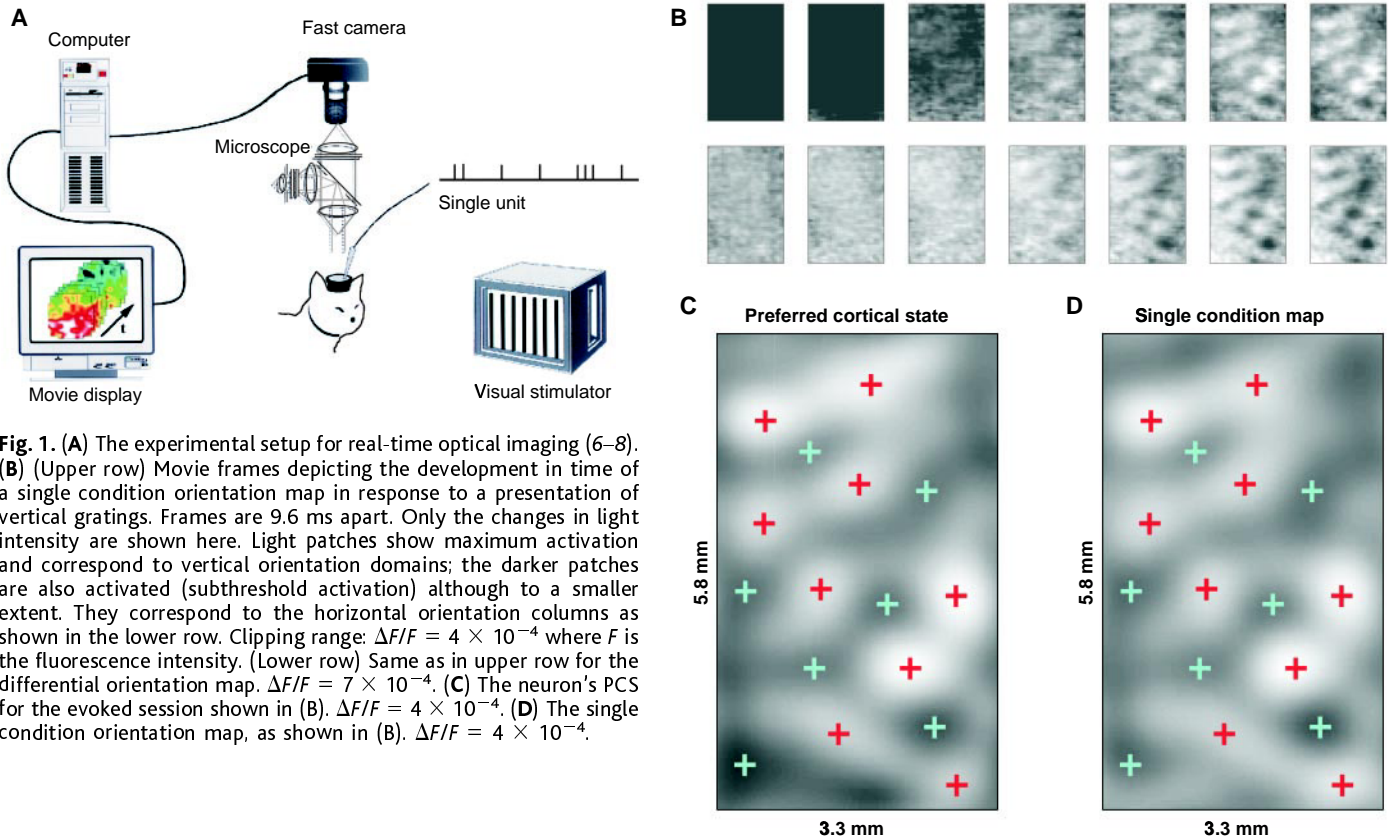


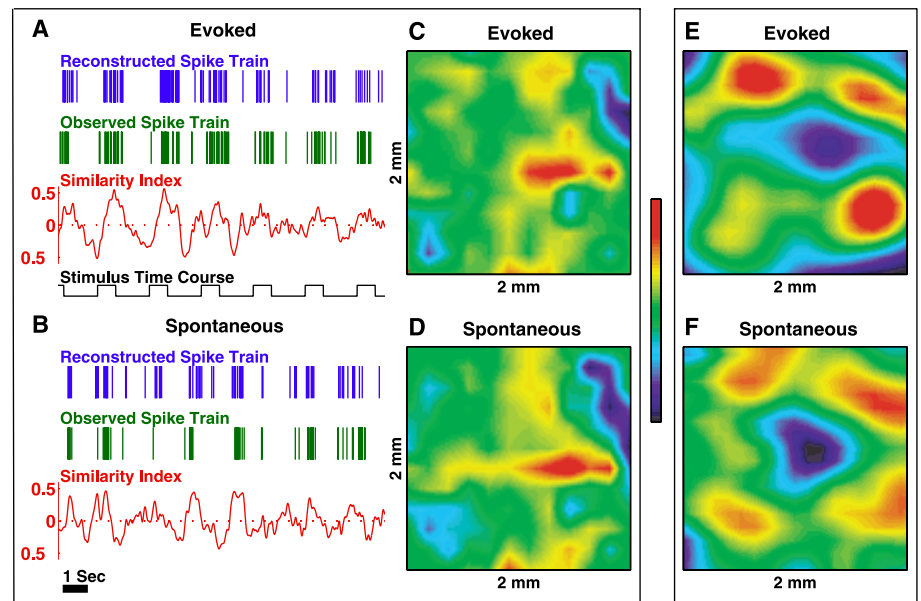
Fig. 1. (A) The experimental setup for real-time optical imaging (6–8). (B) (Upper row) Movie frames depicting the development in time of a single condition orientation map in response to a presentation of vertical gratings. Frames are 9.6 ms apart. Only the changes in light intensity are shown here. Light patches show maximum activation and correspond to vertical orientation domains; the darker patches are also activated (subthreshold activation) although to a smaller extent. They correspond to the horizontal orientation columns as shown in the lower row. Clipping range: $\Delta F/F = 4 \times 10^{-4}$ where F is the fluorescence intensity. (Lower row) Same as in upper row for the differential orientation map. $\Delta F/F = 7 \times 10^{-4}$. (C) The neuron's PCS for the evoked session shown in (B). $\Delta F/F = 4 \times 10^{-4}$. (D) The single condition orientation map, as shown in (B). $\Delta F/F = 4 \times 10^{-4}$.

We then investigated what fraction of spontaneous action potentials were related to the patterns of population activity and to the functional architecture (19). We computed the histogram of correlation coefficients, showing the number of frames occurring for any given value of correlation coefficient, over an entire imaging session (Fig. 3A). The symmetric shape of the histogram, centered on 0, indicates that the state of the network has no bias toward the PCS of

any given neuron. We also calculated the analogous histogram only for the times at which the monitored single neuron fired an action potential (Fig. 3B). We refer to this histogram as the activity histogram. In contrast to the first symmetric histogram shown in Fig. 3A, the activity histogram exhibits a significant bias toward positive correlation values. This implies that a majority of the spontaneous action potentials occur when the population activity is positively corre-

lated with the neuron's functional architecture. In order to obtain the probability that a neuron will fire an action potential at any given value of the correlation coefficient, we divided the bottom histogram by the top one (Bayes rule), which resulted in a steadily increasing function past a certain threshold. To obtain the predicted instantaneous firing rate of a neuron, we further divided this probability by the duration of the time frame (Fig. 3C). At low values of correla-

Fig. 2. Relation between the action potentials of a single neuron and the population state of the network. (A) Black trace: stimulus time course. Red trace: correlation coefficient of the instantaneous snapshot of population activity with the PCS pattern. Green trace: observed spike train of evoked activity with the optimal orientation for that neuron. Blue trace: reconstructed spike train (16). The similarity between the reconstructed and observed spike trains is evident. Also, strong upswings in the values of correlation coefficients are evident each time the neuron emits bursts of action potentials. Every strong burst is followed by a marked downswing in the values of the correlation coefficients. (B) The same as (A), but for a spontaneous activity recording session from the same neuron (eyes closed). (C) The neuron's PCS, calculated during evoked activity and used to obtain both (A) and (B). (D) The cortical state corresponding to spontaneous action potentials. The two patterns are nearly identical (correlation coefficient 0.81). (E and F) Another example of the similarity between the neuron's PCS (E) and the cortical state corresponding to spontaneous activity (F) from a different cat obtained with the high-resolution imaging system (correlation coefficient 0.74). Clipping range: $\Delta F/F = 1 \times 10^{-4}$.



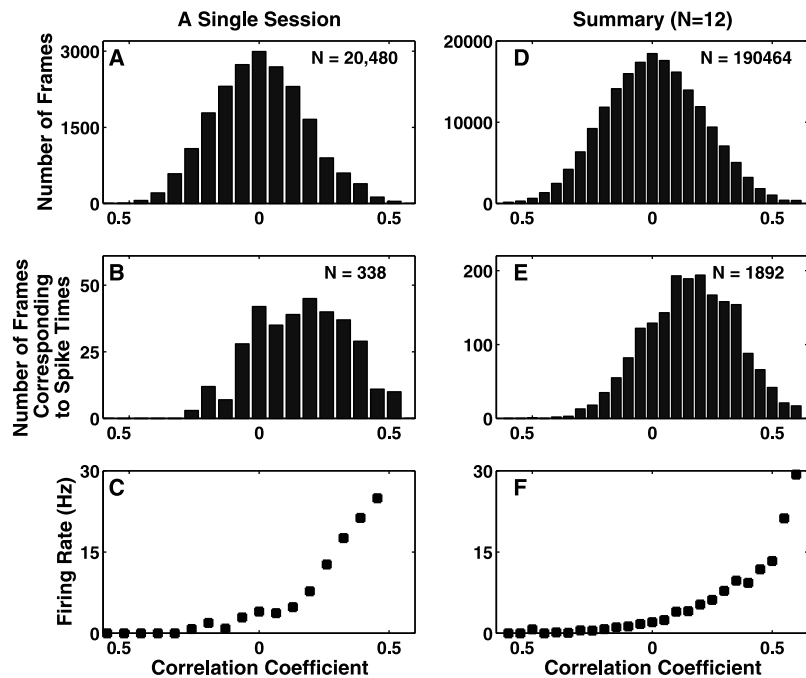


Fig. 3. (A) Histogram of the values of correlation coefficients between the instantaneous state of the spontaneous population activity and the PCS for all 20,480 time samples, for the same recording session as shown in Fig. 2B. (B) The corresponding activity histogram computed only for selected time samples when an action potential was recorded. (C) The predicted instantaneous firing rate of a neuron, given a specific correlation coefficient (squares). (D to F) Same as (A) to (C). Summary of all data from 12 recording sessions in five cats.

tion coefficients, the firing rate is practically zero, and above a certain value it increases monotonically. This graph implies that a neuron's instantaneous firing rate is higher, the more similar the instantaneous population activity pattern is to its functional architecture. Similar results were obtained in five different cats (Fig. 3, D to F). On average, the bias of the activity histogram was 80%, namely 80% of spikes concurred with positive correlation coefficients. The same analysis performed over recording sessions during which the neurons were driven by a visual stimulus with optimal orientation produced similar results.

The fact that nearly the same population state occurs during both spontaneous and evoked activity of a cortical neuron suggests that in the absence of stimulation, the cortical network wanders through various states represented by coherent firing of different neuronal assemblies. When the network activity happens to be in a particular state, neurons with a preference for this state will have the highest firing rate. When a stimulus is presented, it will quickly push the network from whichever state it was in, into the neuron's PCS, which in turn represents the stimulus. The similarity between the underlying functional architecture and the neuron's PCS suggests not only a significant degree of coherent activity in a given cortical orientation column at the recording site, but also coherent activation of distant functional domains with similar tuning properties over a large cortical area. This synchronicity during spontane-

ous activity is presumably mediated by the long-range horizontal cortical connections (20). The results presented here also suggest that orientation domains tuned to different orientations will show a lower level of spike synchronicity during ongoing activity. In the absence of a stimulus, the transitions between cortical states are probably affected by feedback inhibition (21), the dynamic properties of cortical connections (22), or spike frequency adaptation (23). In the awake animal input from either lower or higher areas (24) may affect the cortical state, which may in turn represent higher levels of cortical processing.

Our results indicate that the spontaneous firing of single neurons is tightly linked to the cortical networks in which they are embedded. The idea of a network is a central concept in theoretical brain research (25), and it is now finally possible to directly visualize the cortical networks and their states in action at high spatiotemporal resolution. It appears that in addition to the fruitful studies of single neurons, it is also important to study their behavior in the context of the entire neuronal network. Exploring cortical states is likely to reveal new and fundamental principles about neural strategies for cortical processing, representations of objects, memories, context, expectations, and particularly about the interplay between internal cortical representations and the sensory input in primary sensory areas.

References and Notes

1. E. Riva Sanseverino, L. F. Agnati, M. G. Maioli, C. Galletti, *Brain Res.* **54**, 225 (1973); A. C. Webb, *Proc. R. Soc. London Ser. B.* **194**, 239 (1976); M. Abeles, *Local Cortical Circuits. An Electrophysiological Study* (Springer-Verlag, Berlin, Heidelberg, New York, 1982); C. R. Legendy and M. Salzman, *J. Neurophysiol.* **53**, 926 (1985).
2. A. Arieli, A. Sterkin, A. Grinvald, A. Aertsen, *Science* **273**, 1868 (1996).
3. W. R. Softky and C. Koch, *J. Neurosci.* **13**, 334 (1993); M. N. Shadlen and W. T. Newsome, *Curr. Opin. Neurobiol.* **4**, 569 (1994); C. van Vreeswijk and H. Sompolinsky, *Science* **274**, 1724 (1996); D. J. Amit and N. Brunel, *Cereb. Cortex* **7**, 237 (1997).
4. H. Noda and W. R. Adey, *Brain Res.* **18**, 672 (1970); A. C. Paisley and A. J. Summerlee, *Prog. Neurobiol.* **22**, 155 (1984); W. J. Freeman and C. A. Skarda, *Brain Res.* **375**, 147 (1985); A. Arieli, in *Information Processing in the Cortex*, A. Aertsen and V. Braitenberg, Eds. (Springer-Verlag, Berlin, Heidelberg, New York, 1992), pp. 123-138; M. Abeles et al., *Proc. Natl. Acad. Sci. U.S.A.* **92**, 8616 (1995); A. Destexhe, D. Contreras, M. Steriade, *J. Neurosci.* **19**, 4595 (1999); I. Lampl, I. Reichova, D. Ferster, *Neuron* **22**, 361 (1999).
5. A. Arieli, D. Shoham, R. Hildesheim, A. Grinvald, *J. Neurophysiol.* **73**, 2072 (1995).
6. A. Grinvald, A. Manker, M. Segal, *J. Physiol.* **333**, 269 (1982); H. S. Orbach and L. B. Cohen, *J. Neurosci.* **3**, 2251 (1983); A. Grinvald, L. Anglister, J. A. Freeman, R. Hildesheim, A. Manker, *Nature* **308**, 848 (1984); A. Grinvald, E. E. Lieke, R. D. Frostig, R. Hildesheim, *J. Neurosci.*, **14**, 2545 (1994).
7. Recent advances, including the design of improved voltage-sensitive dyes providing a 10- to 30-fold improvement in signal-to-noise ratio (D. Shoham et al., *Neuron*, in press), the development of a high-resolution fast camera [T. Iijima, G. Matosomoto, Y. Kosokoro, *Neuroscience* **51**, 211 (1992)], and the modification we introduced for in vivo experiments, have enabled us to obtain many of the present results. For an updated review see A. Grinvald et al., in *Modern Techniques in Neuroscience Research*, U. Windhorst and H. Johansson, Eds. (Springer-Verlag, Berlin, Heidelberg, New York, 1999), pp. 893-969.
8. Methods are described in detail in (5). Animals: All surgical and experimental procedures were in accordance with NIH guidelines. To ensure proper levels of anesthesia, the heart rate, electroencephalogram, end-tidal CO₂ volume, and core temperature were monitored throughout the experiment. Experimental methods: We used two fast-imaging systems for optical imaging based on the voltage-sensitive dye with a 12 by 12 photodiode array or the higher resolution Fuji HR-Deltaron system having 128 by 128 pixels (7). Overall, 12 recording sessions were performed with simultaneous recording of a single neuron recorded in each session. We isolated spikes from a single neuron using a Multi-Spike Detector device (MSD) based on template matching (Alpha Omega Engineering, version 3.21). To assure spike separation we performed the standard autocorrelation of the spike train. In experiments with the diode array, we imaged a -2 mm by 2 mm patch of cortex stained with RH795, sampled every 3.5 ms for periods of 70 s. The stimuli were presented for 0.7 s with a 1.3-s interstimulus interval. Cats were anesthetized with Pentothal. In experiments with the high-resolution system, we imaged a 7 mm by 7 mm patch of cortex stained with RH1691, sampled every 9.6 ms for periods of 30 s. Stimuli were presented for 0.2 s with 1-s interstimulus intervals. Cats were anesthetized with Halothane.
9. For this study we selected neurons that fired at least 100 action potentials in a single spontaneous recording session.
10. D. H. Hubel and T. N. Wiesel, *J. Physiol. (London)* **160**, 106 (1962).
11. _____ and M. P. Stryker, *Nature* **269**, 328 (1977); T. Bonhoeffer and A. Grinvald, *Nature* **353**, 429 (1991).
12. In this study we used drifting full-field gratings of optimal orientation for a given neuron (high contrast, 0.2 cycles per degree, duty cycle = 0.2, 18°/s). During

- the interstimulus interval, the same grating was presented but remained stationary in order to avoid a sudden luminance change, which is known to create a transient cortical response exhibiting poor orientation tuning. We verified by single-unit recordings that standing gratings did not evoke cortical activity.
13. We do not rule out, however, the possibility that a few distinct states were mixed in the PCS spatial pattern when this procedure was applied, because single cortical neurons are known to be selective for more than one visual attribute of the stimulus (for example, orientation, direction, and spatial frequency).
 14. This functional map for orientation preference shown in Fig. 1D is defined as a single condition orientation map. Thus far such maps could not be obtained due to the large noise previously associated with voltage-sensitive dye imaging. Only the recent technical advances allowed us to obtain reproducible single condition maps (7). To minimize contributions from the intrinsic signals, the data were filtered above 0.6 Hz and the maps were computed with frames from 100 to 150 ms after stimulus onset, much earlier than the onset of the slow intrinsic signal. Normally, maps are revealed by differential imaging only [T. Bonhoeffer and A. Grinvald, *J. Neurosci.* **13**, 4157 (1993)]. The single condition map was validated by comparing it to the differential orientation maps obtained by using two stimuli of orthogonal orientations (Fig. 1B). In addition, the map was confirmed by imaging based on intrinsic signals. The latter two types of maps can be obtained with a much better signal-to-noise ratio. Therefore, we are confident that the PCS shown here corresponds to the relevant functional architecture.
 15. The evident variability in both single-unit and population responses could have various sources, including the impact of ongoing activity on evoked activity (2) and relatively large noise in these single-trial images. The values of the correlation coefficients warrant a discussion. The fact that correlation coefficients never reach high values (above 0.6) could manifest the mixing of several cortical states in one PCS during the averaging, or it could result from the residual noise in the recording of instantaneous activity patterns. The values of the correlation coefficients should be compared with the highest value that can be obtained for two maps derived under the same experimental conditions. The correlation between two maps produced by the same stimuli on two independent sets of trials was 0.81.
 16. We converted the correlation coefficient between the population activity and the neuron's PCS into a predicted instantaneous firing, as will be explained later (Fig. 3). We then generated a Poisson spike train using this predicted instantaneous rate.
 17. The average correlation coefficient for all five pairs of spontaneous and evoked activity sessions was 0.73 (range 0.65 to 0.81) from five different cats.
 18. We expect that spontaneous activity of a cortical neuron can be predicted by this procedure whenever the neuron has response properties that are common to many other neurons. In other cases where the tuning properties are not that robust, or the neuron is a member of neuronal assemblies possessing different spatial structures, other types of analysis, such as clustering techniques, may be required.
 19. In Fig. 2 we used the neuron's PCS to predict the spike trains. In Fig. 1, C and D, we showed that the PCS and the map of the functional architecture are very similar. Therefore, here we performed the same analysis using both the functional map and the PCS. The results were very similar. In Fig. 3 we show the results based on the functional map.
 20. C. D. Gilbert, *Cereb. Cortex* **3**, 373 (1993); W. Singer, *Int. Rev. Neurobiol.* **37**, 153 (1994); R. Malach, R. B. H. Tootell, D. Malonek, *Cereb. Cortex* **4**, 151 (1994).
 21. A. M. Sillito, J. A. Kemp, J. A. Milson, N. Berardi, *Brain Res.* **194**, 517 (1980); M. Tsodyks and T. Sejnowski, *Network* **6**, 1 (1995); R. Ben-Yishai, D. Hansel, H. Sompolinsky, *J. Comput. Neurosci.* **4**, 57 (1997).
 22. A. M. Thomson and J. Deuchars, *Trends Neurosci.* **17**, 119 (1994); M. Tsodyks and H. Markram, *Proc. Natl. Acad. Sci. U.S.A.* **94**, 719 (1997); L. F. Abbott, J. A. Varela, K. Sen, S. B. Nelson, *Science* **275**, 220 (1997).
 23. B. W. Connors and M. J. Gutnick, *Trends Neurosci.* **13**, 99 (1990); B. Ahmed, J. C. Anderson, R. J.

- Douglas, K. A. Martin, D. Whitteridge, *Cereb. Cortex* **8**, 462 (1998); D. Hansel and H. Sompolinsky, in *Methods in Neuronal Modeling*, C. Koch and I. Segev, Eds. (MIT Press, Cambridge and London, 1998), pp. 499–567.
24. D. J. Felleman and D. C. Van Essen, *Cereb. Cortex* **1**, 1 (1991); P. A. Salin and J. Bullier, *Physiol. Rev.* **75**, 107 (1995); S. Ullman, *Cereb. Cortex* **5**, 1 (1995).
25. D. Amit, *Modeling Brain Function* (Cambridge Univ. Press, New York, 1989); J. Hertz, *Introduction to the Theory of Neural Computation* (Addison-Wesley,

Redwood City, CA, 1991); P. Churchland and T. Sejnowski, *The Computational Brain* (MIT Press, Cambridge, MA, 1992).

26. We thank K. Pawelzik for illuminating discussions and M. Abeles, A. Aertsen, D. Sagi, and H. Sompolinsky for useful comments on the manuscript. Supported by grants from the German Israel Foundation, the Joint German Israeli Research Program, the Wolfson Foundation, Minerva, and Ms. Enoch.

29 June 1999; accepted 25 October 1999

Stimulation of Bone Formation in Vitro and in Rodents by Statins

G. Mundy,^{1*} R. Garrett,¹ S. Harris,² J. Chan,¹ D. Chen,¹ G. Rossini,¹ B. Boyce,³ M. Zhao,¹ G. Gutierrez¹

Osteoporosis and other diseases of bone loss are a major public health problem. Here it is shown that the statins, drugs widely used for lowering serum cholesterol, also enhance new bone formation in vitro and in rodents. This effect was associated with increased expression of the bone morphogenetic protein-2 (BMP-2) gene in bone cells. Lovastatin and simvastatin increased bone formation when injected subcutaneously over the calvaria of mice and increased cancellous bone volume when orally administered to rats. Thus, in appropriate doses, statins may have therapeutic applications for the treatment of osteoporosis.

Diseases of bone loss are a major public health problem for women in all Western communities. It is estimated that 30 million Americans are at risk for osteoporosis, the most common of these diseases, and there are probably 100 million people similarly at risk worldwide (1). These numbers are growing as the elderly population increases. Despite recent successes with drugs that inhibit bone resorption, there is a clear need for nontoxic anabolic agents that will substantially increase bone formation in people who have already suffered substantial bone loss. There are no such drugs currently approved for this indication.

In a search for agents that enhance osteoblast differentiation and bone formation, we looked for small molecules that activated the promoter of the bone morphogenetic protein-2 (BMP-2) gene. We chose this assay because osteoblast differentiation is enhanced by members of the BMP family, including BMP-2 (2), whereas other bone growth factors such as transforming growth factor- β and the fibroblast growth factors (FGFs) stimulate osteoblast proliferation but inhibit

osteoblast differentiation (3). To test the effects of compounds on BMP-2 gene expression, we used the firefly luciferase reporter gene driven by the mouse BMP-2 promoter (-2736/+114 base pairs). The gene was transfected into an immortalized murine osteoblast cell line, which was derived from a transgenic mouse in which simian virus-40 (SV40) large T antigen was directed to cells in the osteoblast lineage (4), and the effects on the promoter were assessed by luciferase activity in the cell lysates.

We examined more than 30,000 compounds from a natural products collection and identified the statin lovastatin as the only natural product in this collection that specifically increased luciferase activity in these cells. The statins are commonly prescribed drugs that inhibit 3-hydroxy-3-methylglutaryl coenzyme A (HMG Co-A) reductase and decrease hepatic cholesterol biosynthesis, thereby reducing serum cholesterol concentrations and lowering the risk of heart attack (5, 6). We also examined the effects of related statins simvastatin, mevastatin, and fluvastatin in this assay. Each of these compounds was maximally effective at 5 μ M and had no effects at concentrations lower than 1 μ M. The increase in luciferase activity was blocked by the immediate downstream metabolite of HMG Co-A reductase, mevalonate (7), which suggests that the effects on bone formation were causally linked to inhibition of this enzyme [although mevalonate may

¹OsteoScreen, 2040 Babcock Road, San Antonio, TX 78229, USA. ²Department of Medicine, ³Department of Pathology, University of Texas Health Science Center, 7703 Floyd Curl Drive, San Antonio, TX 78284-7877, USA.

*To whom correspondence should be addressed. E-mail: mundy@uthscsa.edu